Flat-band ferromagnetism in organic polymers designed by a computer simulation

Yuji Suwa,[1] Ryotaro Arita,[2] Kazuhiko Kuroki,[3] and Hideo Aoki[2]
[1]*Advanced Research Laboratory, Hitachi Ltd., Hatoyama, Saitama 350-0395, Japan*
[2]*Department of Physics, University of Tokyo, Hongo, Tokyo 113-0033, Japan*
[3]*Department of Applied Physics and Chemistry, University of Electro-Communications, Chofu, Tokyo 182-8585, Japan*
(Received 17 July 2003; published 17 November 2003)

By coupling a first-principles, spin-density functional calculation with an exact diagonalization study of the Hubbard model, we have searched over various functional groups for the best case for the flat-band ferromagnetism proposed by R. Arita *et al.* [Phys. Rev. Lett. **88**, 127202 (2002)] in organic polymers of five-membered rings. The original proposal (polyaminotriazole) has turned out to be the best case among the materials examined, where the reason why this is so is identified here. We have also found that the ferromagnetism in the polymer, originally proposed for the half-filled flat band, is stable even when the band filling is varied away from the half filling. All these make the ferromagnetism proposed here more experimentally inviting.

DOI: 10.1103/PhysRevB.68.174419 PACS number(s): 75.10.Lp, 71.20.Rv, 71.10.Fd

I. INTRODUCTION

Materials design to realize desired properties in condensed-matter physics is becoming increasingly realistic. There, computer simulations are an essential part in designing, given high levels of computer performance. Namely, large-scale first-principles calculations should be imperative in narrowing down, or even pinpoint, the right materials for the desired properties and functions out of a wide variety of candidates. Such an approach is especially promising for molecules and nanostructures. While the atom manipulation with scanning tunneling microscopy[1–4] provides new possibilities for materials design, the design of molecules, especially polymers as we focus on here, should be fundamental.

In this context *organic* molecules and polymers are of special interest, since they have versatile structures and chemical properties that can be wider than those found in inorganic materials. Indeed, the discovery of a conducting organic polymer by Shirakawa[5,6] kicked off intensive studies which are paving a new way to organic polymers or oligomers in realizing various functions as molecular-electronics devices such as field-effect transistors[7] or light-emitting diodes.[8]

Organic ferromagnets have also attracted much attention as a challenging target.[9,10] In particular, organic magnets consisting entirely of nonmagnetic elements is of fundamental as well as practical interests. Ordinary ferromagnets consisting of magnetic elements exploit electrons in *d* or *f* orbitals which strongly interact with each other. We can then ask ourselves: can magnetism arise in *p*-electron systems which are weakly interacting? One theoretical possibility is to apply the flat-band ferromagnetism proposed by Mielke and by Tasaki.[11,12] This magnetism arises as an effect of the electron-electron repulsion when the (one-electron) band structure contains a dispersionless band. The mechanism is interesting in many ways, but essential features are, first, the system is totally distinct from the ''narrow-band limit'' in textbooks, since the magnetism occurs when the transfer between different sites is finite.

Second, this is a band ferromagnetism rather than a magnetism arising for localized spins. While there are other possible mechanisms such as the intramolecular Hund's coupling for spins in *p*-orbitals,[9] the flat-band ferromagnetism is distinct in that spins can be carried by itinerant electrons which may be utilized for spin injectors in spintronics.

Here a theoretical remark on the flat-band ferromagnetism is due. The flat-band ferromagnetism was first proposed by Lieb,[13] who considered bipartite lattices (consisting of two sublattices) that have different numbers of *A* sublattice sites N_A and *B* sublattice sites N_B. Lieb proved that when we switch on the electron-electron repulsion (assumed to be short ranged, so that we take the Hubbard model), the ground state should be ferrimagnetic with the magnetization $\propto N_A - N_B$. Quantum chemically, the model, containing $N_A - N_B$ nonbonding molecular orbitals, is similar to Mataga's model.[14] Shima and Aoki[15] then proposed a systematic way to realize such systems as superhoneycomb structures. Mielke[16–18] and independently Tasaki[19] then constructed other flat-band ferromagnetism, which is distinct from Lieb's in that the flat band is constructed from quantum-mechanical interference between the nearest neighbors and further transfers or interference within odd-membered plaquette (so the system is necessarily nonbipartite) and the ground state is now ferromagnetic when the flat band is half filled.

To be more precise, the lattice is required to satisfy what is called the ''local connectivity condition.'' Namely, the flat band is by no means a sufficient condition for ferromagnetism, and the magnetism arises for special lattices on which adjacent ''Wannier'' orbitals *have to* overlap with each other no matter how they are combined to minimize each orbit size. So, while ordinarily a flat band implies a disjointed set of orbits, the orbits are connected in Mielke-Tasaki lattices. This is intuitively why spins align to lower the repulsion energy from Pauli's principle.

In actual materials, it would be very difficult to realize perfectly flat bands, and to make them exactly half filled. For the flatness, a rigorous proof (for Mielke-Tasaki lattice)[20] and numerical simulations[21,22] show that a slight band dispersion does not destroy the magnetism. For the filling, there is a proof[11] and a numerical simulation[21] which reveal that small deviations from half filling are permissible for the ferromagnetism.

With this background, what kind of organic materials are promising for realization of the flat-band ferromagnetism? The hardest part is to realize the connectivity condition. In general we have to consider complex lattices, such as Kagomé,[16] or lattices having distant-neighbor transfers. However, the condition is easier to satisfy on one-dimensional polymers. For example, Mielke-Tasaki model is realized as a chain of triangles.[21,23,24] So we can concentrate on polymers.

Next comes the choice of the monomers that should be polymerized. Even-membered rings such as benzene are disadvantageous in that antiferromagnetic order tends to dominate the magnetism. So we should opt for odd-membered rings, and the chain of triangles mentioned above is an example. Since triangular molecules are scarce, we can focus on polymers based on five-membered rings, such as polypyrrole, polythiophen, etc.

For the computer design, the twofold purpose of the present paper is the following,

(i) to search for the materials that realize the flat band in the manner of Mielke-Tasaki. Since the chain of odd-membered rings is by no means a sufficient (nor necessary) condition for the flat band, this is an important part.

(ii) Next, we should do a first-principles (spin-density functional) band calculation to confirm (a) the flatness of the band and the ferromagnetism in the ground state and (b) whether the magnetism can indeed be interpreted as the Mielke-Tasaki mechanism, for which we have to evoke an electron-correlation calculation (exact diagonalization of the Hubbard model here). (c) We also address the question of how the departure from half filling affects the magnetism in the flat band.

For the first-principles calculation, we have employed the generalized gradient approximation[25] (GGA). Depending on the purpose of each calculation, we have studied either the spin-unpolarized case based on the density-functional theory (GGA-DFT) or the spin-polarized one based on the spin-density functional theory (GGA-SDFT). We have used the plane-wave based ultrasoft pseudopotentials.[26,27] The energy cutoff was taken as 20.25 Ry. The convergence criterion of the geometry optimization was that all of the forces acting on each atom were within 1×10^{-3} Hartree/a.u.

The plan of this paper is as follows. In Sec. II, we describe the search for various materials and show some examples which exhibit possibilities of ferromagnetism. In Sec. III, we show the result for the most promising material, polyaminotriazole, and discuss how the theory for the flat-band ferromagnetism works on this particular material. In Sec. IV, we discuss how the ferromagnetic state is robust against the deviation of the band filling from the half filling.

II. EXAMINED MATERIALS

A. Flat bands in the polymer of five-membered rings

Let us first examine the simple tight-binding model,

$$H=-t\sum_{\langle i,j\rangle} c_i^{\dagger}c_j+\varepsilon_0\sum_{i=2}^{5} n_i+\varepsilon_1 n_1, \qquad (1)$$

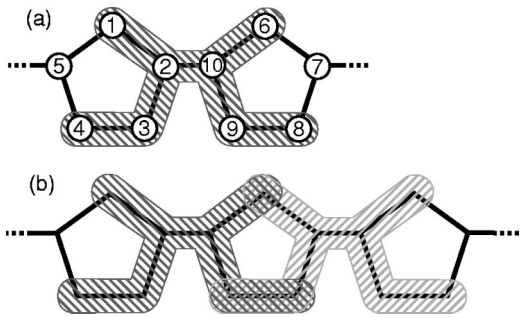

FIG. 1. (a) An eigenfunction that satisfies the connectivity condition. (b) The overlap of the adjacent eigenfunctions.

for a chain of five-membered rings, where we first assume that all the transfer integrals within the ring and those connecting rings have the same t, and the on-site energy at the top of each ring is ε_1 and zero otherwise ($\varepsilon_0=0$). We first consider the half-filled case where one electron per site on average. This is a reasonable assumption when we consider π-orbital networks on such polymers.

Let us start from an observation that Mielke-Tasaki's condition is satisfied when $\varepsilon_1=t$ (>0), not an unrealistic condition. In this case, the third band with $E=0$, i.e., the half-filled band, has flat dispersion. It is heuristic to see how the Mielke-Tasaki eigenfunctions are constructed in this example: the most compact eigenfunction extends over two rings as depicted in Fig. 1(a), where the amplitudes of the numbered sites are given as (1, 1, 0, -1, 0, -1, 0, 1, 0, -1). The fact that the amplitudes at the sites 5 and 7 are zero ensures the localized nature of this eigenfunction. Note that we are not displaying a part of a Bloch function, but the entire eigenfunction. One can also construct another, linearly independent eigenfunction by simply shifting the wave function by one ring distance, where its eigenvalue is the same ($E=0$). So the set of all these eigenfunctions can be a basis for the flat band. Since each eigenfunction extends over the two rings, two neighboring basis functions overlap as shown in Fig. 1(b). One cannot remove such overlaps between the bases no matter how the linear combination of these bases are taken. This overlap is the origin of the ferromagnetic coupling between the electrons in the flat band.

B. Known polymers of five-membered rings

A typical polymer of five-membered rings is polypyrrole. The atomic structure and calculated band structures are shown in Figs. 2(a) and 2(b), respectively. The five-membered rings alternate their directions in this compound, so that the unit cell contains two rings. X point in Fig. 2(b) has $\boldsymbol{k}=(\pi/a,0,0)$, where a is the lattice constant of this unit cell as shown in Fig. 2(a). Because of the doubled unit cell, most of the bands are folded at X. For directions perpendicular to the chain (y,z), we have taken a cell size large enough to avoid interchain interactions. We can see that polypyrrole has no flat bands around the Fermi energy, not surprisingly since the chain of odd-membered rings is by no means sufficient as stressed.

We have also looked at other typical polymers of five-membered rings, including polythiophen (where an N-H

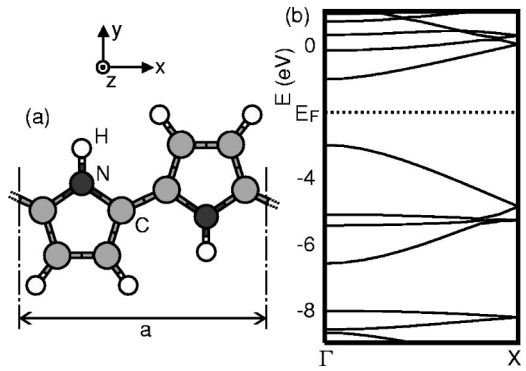

FIG. 2. (a) Atomic structure of polypyrrole. The structure repeats itself to the right and left. (b) The (GGA-DFT) band structure of polypyrrole.

block in polypyrrole is replaced with an S atom) and polytriazole (where all the C-H blocks in polypyrrole are replaced with N atoms). However, their band structures have no flat bands, either.

C. Designing the polymer

This is exactly where the *designing* comes in. Our strategy consists of two approaches. One is to replace H atom bound to N atom at the top of the ring with various kinds of bases. According to the tight-binding calculation described in the preceding section, the on-site energy ε_1 of the top of the ring should be higher than that of C atoms to have a flat band. Because the on-site energy of N is expected to be lower than that of C, the first attempt should be the replacement of the N atom with other elements having higher on-site energies. However, that should be difficult if one wants to retain the existence of the π orbital with a single-electron occupation on it. Therefore, we have opted for controlling the on-site energy by replacing the H atom with other functional groups, by leaving the N atom intact.

Alternatively, we can replace C-H blocks on the bottom edge of the pentagons [3, 4, 8, 9 in Fig. 1(a)] with N atoms, where the lowering of the on-site energies of the bottom of the ring may effectively realize the required condition. In other words, we use polypyrrole and polytriazole as the platform to modify either the top or the bottom of the ring. Since it is not obvious which approach should be better, we consider both platforms for all the substituents considered here.

Substituents we have tested are sodium (Na), potassium (K), chlorine (Cl), fluorine (F), cyanogen (CN), nitro (NO_2), sulfate (SO_4), carboxyl (COOH), amino (NH_2), methyl (CH_3), and hydroxyl (OH). For all these candidates, we have performed first-principles (GGA-DFT) optimization of atomic structures, and obtained their band structures. Most of them have no flat bands around E_F, but some of them have turned out to have flat bands. For these we have performed further (GGA-SDFT) first-principles optimizations under the doping condition to make the flat-band half filled.

First, we have examined single atoms (alkali metal or halogen) as substituents. This is motivated by the fact that small substituents may be better than larger ones, because a bulky group at the top of the ring may introduce a coupling

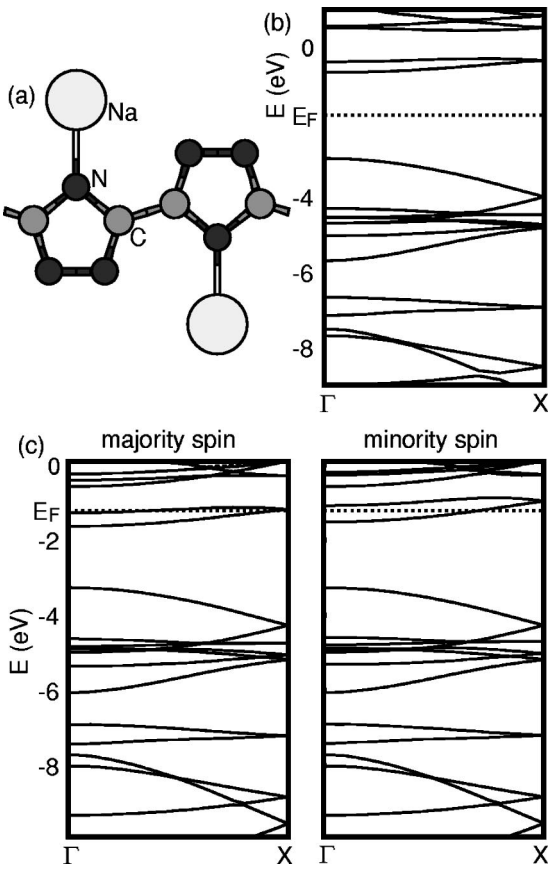

FIG. 3. For poly-sodium-triazole the optimized atomic structure (a), the band structure when undoped (spin unpolarized) (b), and when doped (spin polarized) (c) are shown.

(transfer) with the adjacent ring, which would destroy the basic assumption that the adjacent rings are connected by one bond to satisfy Mielke-Tasaki's condition.

In order to raise the on-site energy of the top of the ring, we have first considered an alkali-metal atom, Na, because of its low electron affinity. Figure 3(a) shows the atomic structure of poly-sodium-triazole, where hydrogen atoms in polytriazole are replaced by sodium atoms. Figure 3(b) shows the band structure, where one can see that a nearly flat band exists above the Fermi energy. Absence of any unnecessary bands between the flat band and E_F is favorable, because we can dope carriers into the flat band without any complications.

We have also examined the Na-substituted polypyrrole, and obtained a similar band structure. However, in this case the flat band above E_F is much closer to a dispersive band below E_F, which can introduce unwanted interband interactions. As for the alkali-metal we have also considered potassium, but the case of Na has turned out to be better.

We move on to the doping. First, the flat bands always appear as a pair of bands folded at X point, except for the case of antiferromagnetic ordering. Therefore, we make the flat-band half filled by doping two carriers per unit cell into the pair of flat bands. Namely, one carrier is doped for each ring. In poly-sodium-triazole, we have considered the doping of two electrons per unit cell. Here we realize the doping

condition by increasing the number of electrons with a uniform positive background charge for charge neutrality.

After a geometrical optimization of doped poly-sodium-triazole, we have calculated the spin-dependent (GGA-SDFT) band structure in Fig. 3(c). We can see that the number of occupied states differs between major and minor spins, which means that the system is ferromagnetic. It should be noted that (the pair of) the flat band is not entirely spin-split. The difference of the number of spins is 0.65 per unit cell. The spin polarization is smaller than the full polarization (2.0). We also found that the total energy (per unit cell throughout this paper) of the ferromagnetic (F) state is lower by 12 meV than that of the paramagnetic (P) state. We could not find antiferromagnetic (AF) solution even when we started geometry optimization from an AF electronic state. So the F state is the most stable in this material, but is only slightly lower in energy than the P state.

The reason why this material gives such an insufficient result in spite of the existence of the nearly flat band should be sought in the nature of the flat-band's wave function. We found that the half-filled flat band here is made of an orbital localized around the Na atom, so it does not satisfy the local connectivity condition. This should be the reason why the stability of the F state is weak, while the finite spin-polarization in GGA-SDFT should be a narrow-band effect rather than a much more robust Mielke-Tasaki effect. Indeed, the difference between the weak ferromagnetism here and a robust ferromagnetism in polyaminotriazole, shown later, is a good demonstration of the importance of the local connectivity condition, hallmark of the flat-band ferromagnetism.

Now we digress a bit, and consider the contrary case of an atom having high electron affinity such as a halogen, e.g., fluorine atom, which might be heuristic. Figure 4(a) shows the atomic structure of polyfluoropyrrole, where the fluorine atoms are substituted for hydrogen atoms bound to nitrogen atoms in polypyrrole. Figure 4(b) is the band structure obtained by spin-unpolarized (GGA-DFT) calculation. We find a flat band which lies just in between two dispersive bands below E_F. Because of this the doping greater than one carrier per unit cell is required.

So we consider making the flat-band half filled by doping four holes per unit cell. Here, two holes are necessary to make the dispersive band just below the Fermi level empty, and two holes are necessary to make the folded flat-bands half filled. Figure 4(c) shows spin-dependent band structure after the geometry optimization under the doping condition. The system is seen to be ferromagnetic. The difference of the number of spins per unit cell is just 2.0, while the flat band shifts upward (downward) for the minority (majority) spins. One problem of this material, however, is that a doping twice as large is necessary. Furthermore an AF state, obtained by starting the geometry optimization from an antiferromagnetic state, has a total energy 21 meV lower than that of F state. Replacing the fluorine atom with a chlorine atom results in a band structure similar to the case of fluorine.

We move on to functional groups as substituents to search further possibilities. We have considered an example, poly-hydroxytriazole, where H atom in polytriazole is replaced by OH with a low electron affinity. Although a pair of slightly

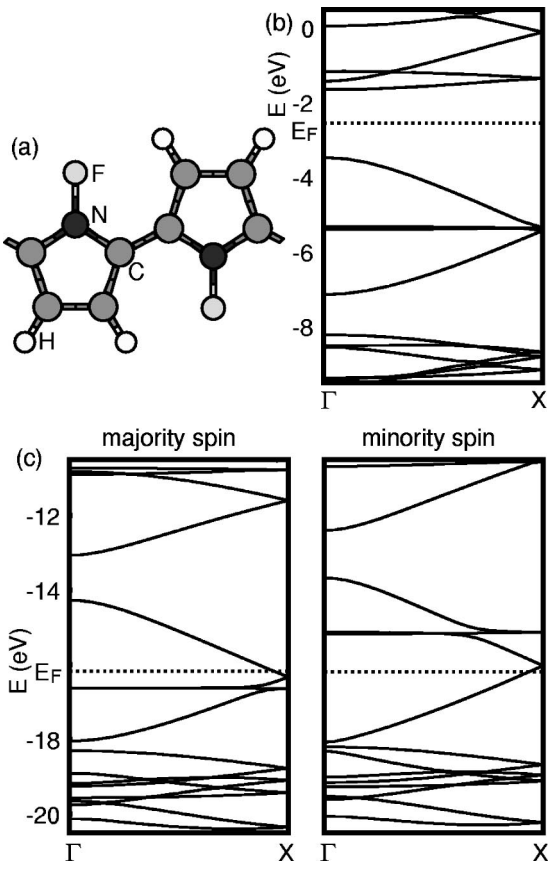

FIG. 4. For polyfluoropyrrole the optimized atomic structure (a), the band structure when undoped (spin unpolarized) (b), and when doped (spin polarized) (c) are shown.

dispersive bands exist just below E_F, these bands, when doped with two holes per unit cell, become mixed with dispersive bands underneath. As a result, the difference of the number of spins in the F state is only 0.39 per unit cell, and the paramagnetic state is more stable than the F state by 3 meV.

Figure 5(a) is the atomic structure of polyaminopyrrole, where H atom bound to N atom in polypyrrole is replaced by NH_2, whose electron affinity is low. In the band structure, Fig. 5(b), one can find a pair of flat bands below E_F. Its lower half is flat while the upper half is slightly dispersive.

We have then doped two holes per unit cell. The band structure after geometry optimization is shown in Fig. 5(c). The difference of the number of spins is 1.0 per unit cell. As one can see from Fig. 5(c), the Fermi level intersects the middle of the pair of flat bands. Although the lower part of the pair of flat bands is quite flat, the dispersion of the upper half part is too large, and only lower half part seems to work as a flat band. The total energy of paramagnetic state in this material is found to be 65 meV higher than that of ferromagnetic state, while an AF solution does not exist, so the F state is the most stable.

All other substituents tested here except for the one in the following section have turned out to be inappropriate. In most of those materials, the band which we expect to be flat is either too dispersive or too deep. For the remaining ones,

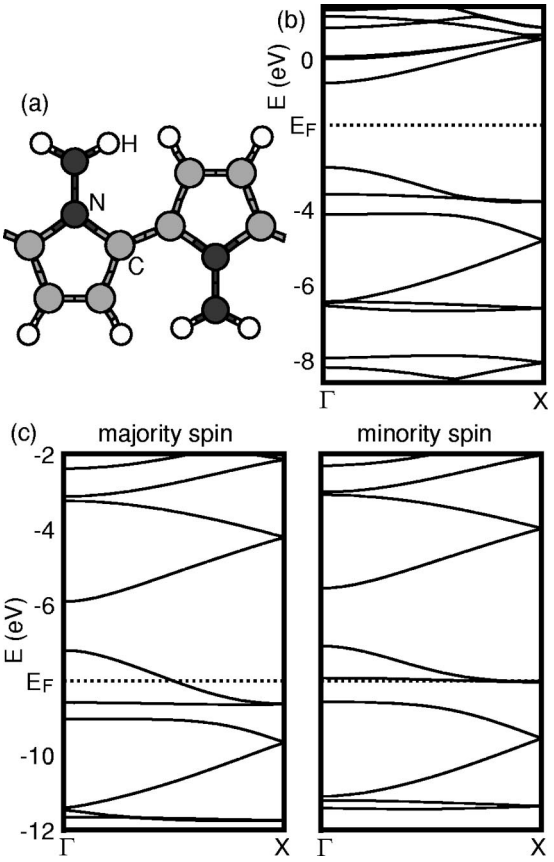

FIG. 5. For polyaminopyrrole the optimized atomic structure (a), the band structure when undoped (spin unpolarized) (b), and when doped (spin polarized) (c) are shown.

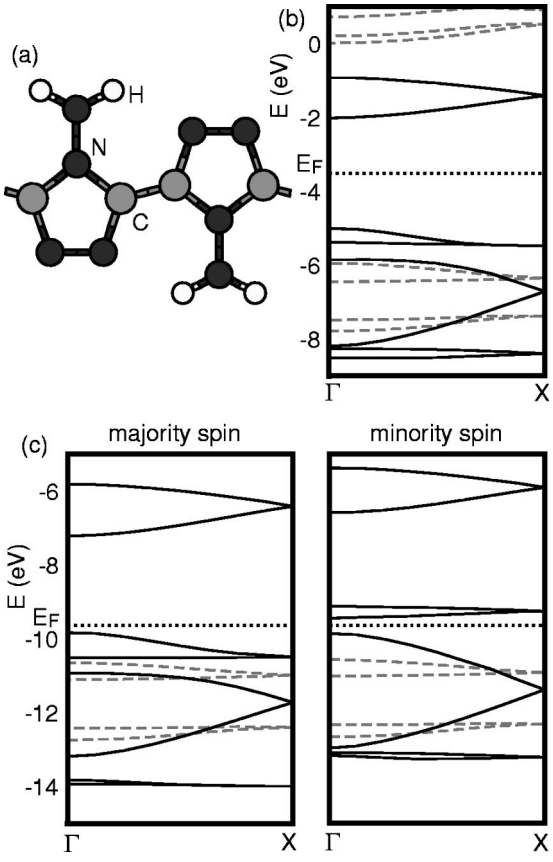

FIG. 6. For polyaminotriazole the optimized atomic structure (a), the band structure when undoped (spin unpolarized) (b), and when doped (spin polarized) (c) are shown. The bands having π (σ) character are indicated by solid (dashed) lines.

band structures are qualitatively similar to the examples described in this section. Polyaminotriazole, discussed in the following section, also gives qualitatively similar results to polyaminopyrrole shown in this section, but quantitatively much better.

III. POLYAMINOTRIAZOLE

A. First-principles calculation

The best candidate for ferromagnetic organic polymer among the materials we have considered is polyaminotriazole.[28] Figure 6(a) shows the atomic structure of polyaminotriazole, where H atom in polytriazole is replaced with NH_2. The difference between polyaminopyrrole shown in the last section and this material is whether the platform is polypyrrole or polytriazole, i.e., the C-H blocks in the bottom of the ring are replaced with N atoms. The band structure of the polyaminotriazole, shown in Fig. 6(b), is similar to that of Fig. 5(b), but the dispersion of the upper half of the pair of flat bands is smaller and the separation from dispersive bands below is greater than that of Fig. 5(b). These features are desirable for the flat-band ferromagnetism.

After the optimization of the atomic structure under the doping condition of two holes per unit cell, the spin-dependent band structure is calculated and shown in Fig. 6(c). The result hits on the ideal situation—the pair of flat bands are made half filled, and as a result, fully occupied by majority spins while totally unoccupied by minority spins. Reflecting this situation the difference of the number of spins is the desired 2.0 per unit cell.

In this material, we found a metastable antiferromagnetic state, whose band structure is shown in Fig. 7. This is calcu-

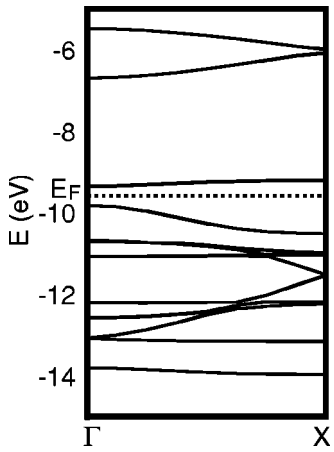

FIG. 7. A band structure for a metastable antiferromagnetic state in polyaminotriazole.

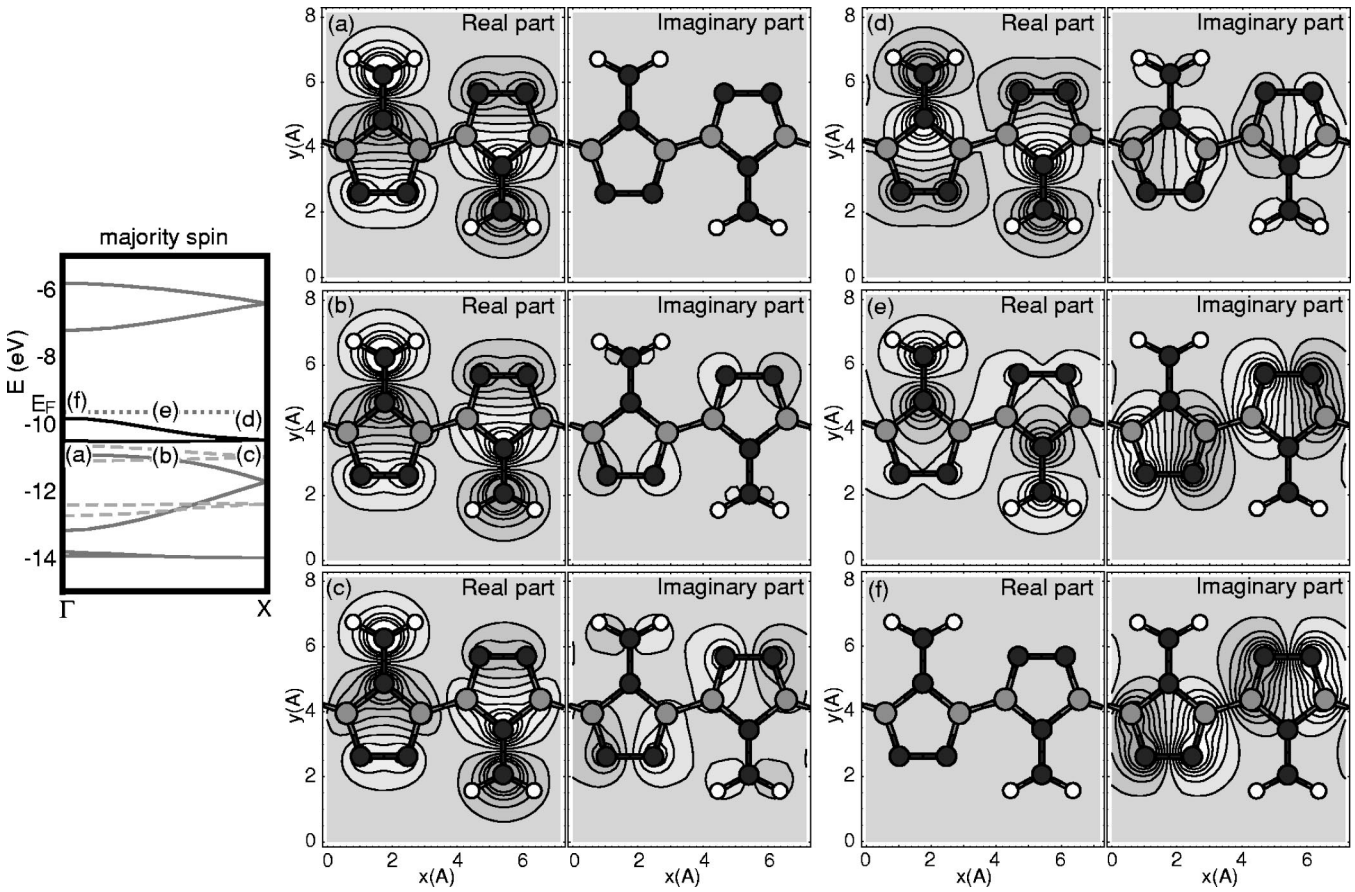

FIG. 8. Wave functions of the polarized lower band (a)–(c) and upper band (d)–(f) of polyaminotriazole. (a), (f) have $k_x=0$ (Γ); (b), (e) have $k_x=\pi/2a$; and (c), (d) have $k_x=\pi/a$ (X) as the inset indicates.

lated with GGA-SDFT, but the resulting band structures for up and down spins are the same, while the wave functions for up and down spins are arranged alternately on the chain of rings. This means that, while we have avoided intraring AF instability by choosing five-membered rings, an interring AF can exist as a metastable state. The upper and lower parts of the flat band folded at X are separated with E_F lying in between. The AF state is found to be 52 meV higher in energy than the F state. Paramagnetic state is even higher (by 384 meV) than the F state. Therefore F state is the most stable in this material.

Let us discuss how the system achieve the flat-band ferromagnetism by comparing the wave functions of the flat band obtained by first-principles calculation with the calculation in the tight-binding model. Figure 8 shows the majority-spin's wave functions in the pair of flat bands just below the Fermi level in Fig. 6(c). While the phases of the wave functions can be taken arbitrarily, we choose them for clarity in such a way that the wave functions of the lower (upper) bands at Γ point [Figs. 8(a) and 8(f)] are real (pure imaginary), while the phase changes continuously along the dispersion. If we first look at the real part, typically for Fig. 8(a), the wave function for each monomer (aminotriazole) has two nodal lines which divide the amplitude into three parts, corresponding to NH_2, C-N-C, and N-N blocks. For the imaginary part, typically for Fig. 8(f), the wave function has one nodal line, which divides the amplitude into two, consisting of two C-N blocks. The two wave functions at Γ, which are orthogonal, become mixed at intermediate k points.

B. Tight-binding model

In order to capture the essence of the flat band, here we introduce a tight-binding model to represent the π-orbital's network. Figure 9(a) shows its band structure. The parameters of the model displayed in Fig. 9(b) are fitted so as to reproduce Fig. 6(b). Obtained values are $t_{\mathrm{CN}}=t_{\mathrm{CC}}=t_{\mathrm{f}}=2.5$ eV, $t_{\mathrm{NN}}=3$ eV, $\varepsilon_0=-1.4$ eV, and $\varepsilon_1=-0.5$ eV. One can see that the tight-binding band [Fig. 9(a)] excellently agrees with the π bands obtained by first-principles calculation [solid lines in Fig. 6(b)].

Figure 9(c) shows the tight-binding wave function of the eigenstate corresponding to that in Fig. 1(a). In this material, one site is added to the top of the ring which represents a nitrogen atom of NH_2. The open and closed circles indicate the sign of the wave function, respectively, and their size amplitudes. This wave function satisfies the local connectivity condition.

Here it should be noted that the substitution of NH_2 for H not only raises the on-site energy of the top of the ring but also introduces an extra π orbital of the N in NH_2. The existence of the extra site completely changes the connectiv-

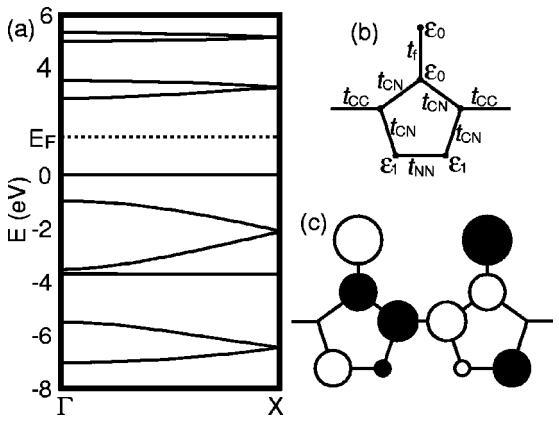

FIG. 9. (a) Band structure in the tight-binding model, (b) defines the tight-binding parameters, while (c) depicts the eigenfunction which satisfies the connectivity condition. The open (solid) circles indicate the positive (negative) wave function, while their size indicates the amplitude.

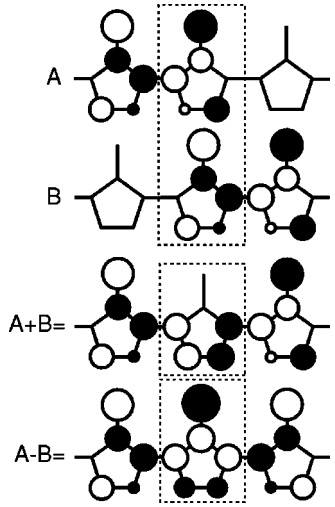

FIG. 11. Schematic linear combinations of the neighboring eigenfunctions.

ity condition, so that we have no longer to satisfy $\varepsilon_1 = t > 0$, which has turned out in the present study to be rather difficult condition to realize.

Figure 10 shows k dependence of the tight-binding wave functions of the flat band. For clarity the k space is extended to the second Brillouin zone, so the left and right halves of the figure represent the wave functions of the lower and upper parts of the pair of flat bands, respectively. Phase factors are chosen again for clarity as in Fig. 8. On the Γ points at the left and right edges of the figure, the wave function becomes real and pure imaginary, respectively. These wave functions are displayed in the inset of Fig. 10, where it should be noted that we display a part of the periodically extending Bloch functions, in contrast to Fig. 9(c) which shows the whole eigenfunction.

One can see that the symmetry and the character of the wave functions shown in Fig. 10 are similar to those in the first-principles calculation (Fig. 8). These wave functions can be constructed by linear combinations of the eigenfunctions shown in Fig. 9(c). Figure 11 illustrates how the linear combination of the localized eigenfunctions provides the Bloch

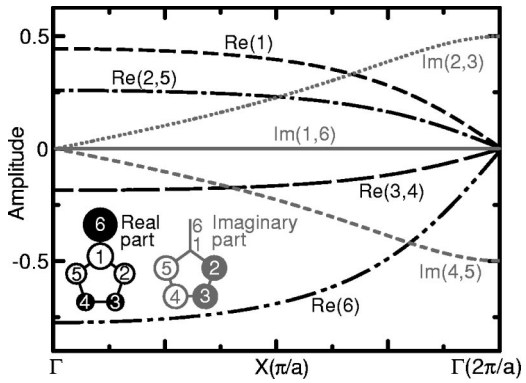

FIG. 10. k dependence of the wave functions in the tight-binding model. The label "Re(2,5)" indicates that the line represents the real part of the wave function at the site 2 and 5, where the numbering of the sites is shown in the inset.

function. When the two neighboring eigenfunctions, A and B, are added, the sum at the ring on which they overlap (enclosed by dotted lines) forms the shape of the imaginary-part wave function as shown in the inset of Fig. 10. When subtracted, it forms the shape of the real-part wave function. The entire imaginary- and real-part wave functions are constructed by the summation of all the localized eigenfunctions $(A+B+C+D+\cdots)$ and the staggered summation $(A-B+C-D+\cdots)$, respectively. The real-part and imaginary-part wave functions are orthogonal. The gradual mixing of these two orthogonal wave functions as k is changed is the very character of the Mielke-Tasaki flat band, which should never occur on an ordinary flat band.

C. Comparison with the Hubbard model

Having constructed the tight-binding model we proceed to the question of whether the ground state is spin polarized in the presence of the Hubbard interaction, $\mathcal{H}_U = U\Sigma_i n_{i\uparrow} n_{i\downarrow}$. In Fig. 12 we show the phase diagram against U and ε_1 obtained from an exact diagonalization of a 12-site (2 rings) Hubbard model for $t_0 = 2.5$ eV and various values of $t_{\mathrm{NN}} = 3.0-4.0$ eV. As indicated in the inset, ε_0 is chosen throughout to satisfy the condition for the flat band,

$$\varepsilon - \varepsilon_1 = (1-\varepsilon)(t_{\mathrm{NN}}^2 - (\varepsilon-\varepsilon_1)^2) - t_{\mathrm{NN}},$$

$$\frac{\varepsilon-\varepsilon_1+t_{\mathrm{NN}}}{1-\varepsilon} = -\frac{t_{\mathrm{NN}}}{\varepsilon_0-\varepsilon} - t_{\mathrm{NN}}(\varepsilon-\varepsilon_0), \qquad (2)$$

where ε is the eigenenergy of the flat band and $t_{\mathrm{CN}} = t_{\mathrm{CC}} = t_0$ ($=1$ here) is assumed for simplicity. We can see that we have indeed a ferromagnetic phase unless the repulsion is too strong (i.e., $U < U_c$ with $U_c = 2 \sim 5$ eV). While we cannot increase the system size for an exact diagonalization calculation, our preliminary quantum Monte Carlo calculation confirms that two unit cell is sufficient to roughly determine the ferromagnetic phase boundary. Physically, the peculiar destruction of the ferromagnetism above $U > U_c$ is a hall-

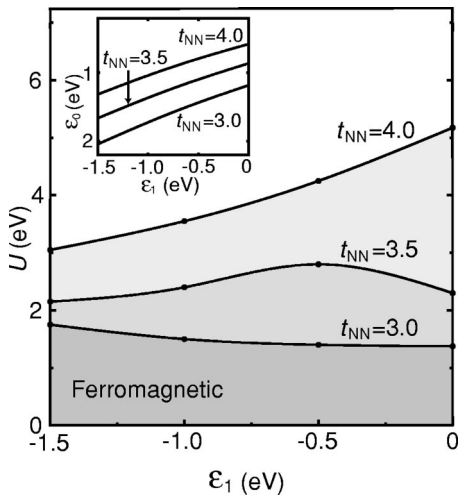

FIG. 12. Stability of the ferromagnetic phase obtained from an exact diagonalization of the Hubbard model.

mark of the Mielke-Tasaki magnetism when the flat band lies in between dispersive ones rather than at the bottom.[22]

IV. DEVIATION FROM THE HALF-FILLED FLAT BAND

A. Comparison of the total energies

In order to realize ferromagnetism in the materials we proposed here, carriers have to be doped into the flat band. We can consider several possible methods to achieve this such as field effect doping,[29] photoinduced carrier injection,[30] as well as chemical doping. The first two are now attracting much attention in molecular electronics, but they are very recent techniques and may need further developments. We can instead concentrate on the chemical doping, where the polymers are crystallized along with the accepters, and we found it feasible. Details are presented elsewhere.[31]

Now, if the flat-band ferromagnetism can occur not only just at the half filling but also away from that, this would make the chemical doping much easier. So we have to know how robustly the ferromagnetism survives when the filling of the flat band deviates from just half filled. Although there is a proof[11] and a numerical study[21] for a Mielke-Tasaki lattice which show that slight deviations do not wash out the ferromagnetism, those conclusions may not be simply applied to other models. For the present model, calculations taking full account of the electronic correlation such as the exact diagonalization of the Hubbard model would be unsuitable, because changing the number of electrons in small systems corresponds to too big a change in the filling. We have instead performed an SDFT calculation, because it can handle the fractional number of electrons (per unit cell) if a uniform background charge is introduced.

At this point we can note the following. In SDFT electronic correlations are not fully taken into account, so we can question whether the flat-band ferromagnetism may be described within the SDFT framework. This problem has been addressed in our previous publication,[28] where SDFT and exact diagonalization of a Hubbard model have given qualitatively consistent results. This is not surprising, since one of

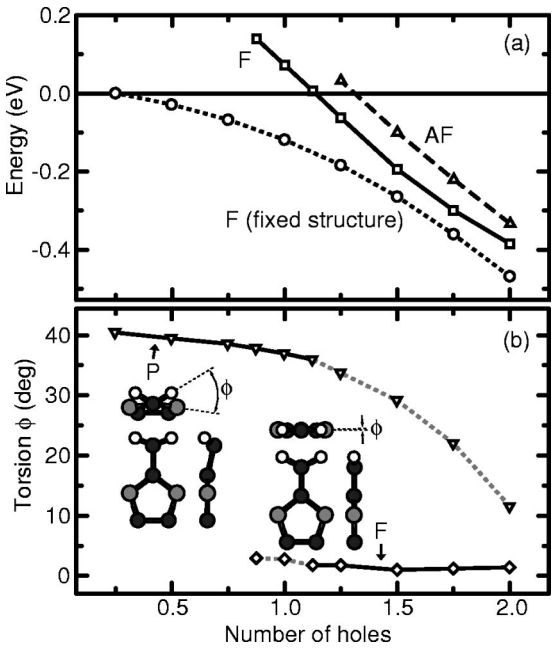

FIG. 13. Doping dependence of (a) the total energy (relative to the paramagnetic state) of F (solid line), AF (dashed line), and F (fixed structure, dotted line, see text) states measured from that of P state and (b) torsion angle of C-N-N-H in F (diamonds) and P (reversed triangles) states. Stable states are connected by a solid line, while metastable states by a dotted line. Insets show front, side, and top views of the atomic structure of the aminotriazole in P and F states.

the remarkable features of the flat-band ferromagnetism is that the magnetism exists over the whole range (infinitesimal $<U<\infty$) of the interaction as proved rigorously, so the weak-U case (for which the methods such as SDFT is meant to be applicable) crosses continuously over to strong-U case. As far as the on-site repulsion is not too strong, the comparison between the gain of the exchange-correlation energy by spin polarization (F state) and the gain of the band energy by forming AF order (or equivalently, a spin-density wave with the periodicity of two five-membered rings) accompanied by a lattice relaxation should predominantly determine which state is stable. These two energies can be accurately estimated by SDFT calculations. Therefore, we expect here that SDFT can serve our purpose, to see the band-filling dependence of the total energies of F, AF, and P states.

Figure 13(a) shows the band-filling dependence of the total energies of the F and AF states measured from that of the P state in poly aminotriazole. The half filling corresponds to the number of holes $n_h=2.0$. The results for F, AF, and P are obtained by fully relaxing the atomic geometry for each electronic state. It can be seen that F state is stable in the range $1.1<n_h\leqslant 2.0$, while P state is stable for $n_h<1.1$. In the region where F is stable, AF is found to be metastable, while in the P region, $n_h<1.1$, no AF state is found. This result shows that the ferromagnetism in this material is robust, even down to the quarter filling ($n_h\simeq 1$), against the deviation from the half filling. The result that quarter filling is acceptable greatly relaxes the difficulty in doping.

B. Correlation with the atomic configuration

Since the polymer proposed here has functional groups, we should also examine how the three-dimensional atomic configuration affects the band-filling dependence. Namely, all the atoms do not lie on a plane: in polyaminotriazole two hydrogen atoms in NH_2 in the undoped polymer lie out of the plane of the rings, while all the atoms are coplanar in the half-filled polyaminotriazole. We can more closely look at the torsion angle ϕ defined as the angle with which C-N-N-H atoms are connected. Figure 13(b) shows the dependence of the torsion angle on n_h for the P and F states, respectively. From Figs. 13(a) and 13(b), one can see that the breakdown of the ferromagnetism with the decrease in the number of holes is accompanied by a change in the atomic configuration.

Does this has a quantum-chemical implication? At the half filling ($n_h=2.0$) all the atoms become co-planar, where the N atom of the NH_2 base has sp^2 hybridized orbitals, forming chemical bonds with two H atoms and a N atom at the top of the ring. The network of the π orbitals in polyaminotriazole is formed by those of the rings and that of NH_2's. When the number of holes is decreased and becomes $n_h<1.1$, the N atom of the NH_2 forms sp^3 hybridized orbitals, i.e., the π orbital at NH_2 disappears. Since the chemical bonds to the N atom and two H atoms are formed in the three directions of sp^3, leaving one lone pair, NH_2 has a three-dimensional structure. This time, the network consists of five π orbitals of the rings and a sp^3 hybridized orbital of the lone pair. This change should work to destroy the flat-band formation, Eq. (2). This should be why F state prefers a flat geometry while P state a non flat geometry.

To see what part of the energy affects the change in the stable state when n_h is varied, we have calculated the energy difference between the F and P states by fixing the atomic structure to the optimum one for the F state at $n_h=2.0$. The result is plotted as a dotted line in Fig. 13(a). This shows that the value is negative over the whole range plotted here, which indicates that the *electronic* part of the total energy favors F state for the whole range of the filling of the flat band. Therefore, the jump in the stable state at $n_h=1.1$ is related to the change in the structure, especially of NH_2. If we can find a material in which there is no such change in the atomic structure, we can expect the ferromagnetism persists even for the region less than quarter filled if the parameter values are similar.

In summary, the present work describes an example of materials design from first principles for the purpose of realizing flat-band ferromagnetism in organic polymers. We have found a promising material, polyaminotriazole, for which why it is the best and the robustness of the ferromagnetism has been discussed.

ACKNOWLEDGMENTS

We would like to thank T. Hashizume, B.-K. Choi, M. Ichimura, and J. Yamauchi for fruitful discussions. We are also indebted to H. Nishihara and Y. Yamanoi for discussions on the chemistry of polymers. This study was performed through Special Coordination Funds for Promoting Science and Technology of the Ministry of Education, Culture, Sports, Science and Technology of the Japanese Government. The first-principles calculations were performed with TAPP (the Tokyo ab-initio program package).

[1] D.M. Eigler and E.K. Schweizer, Nature (London) **344**, 524 (1990).
[2] T.C. Shen, C. Wang, G.C. Abeln, J.R. Tucker, J.W. Lyding, P. Avouris, and R.E. Walkup, Science **268**, 1590 (1995).
[3] T. Hashizume, S. Heike, M.I. Lutwyche, S. Watanabe, K. Nakajima, T. Nishi, and Y. Wada, Jpn. J. Appl. Phys., Part 2 **35**, L1085 (1996).
[4] T. Hitosugi, S. Heike, T. Onogi, T. Hashizume, S. Watanabe, Z.-Q. Li, K. Ohno, Y. Kawazoe, T. Hasegawa, and K. Kitazawa, Phys. Rev. Lett. **82**, 4034 (1999).
[5] T. Ito, H. Shirakwa, and S. Ikeda, J. Polym. Sci., Polym. Chem. Ed. **12**, 11 (1974).
[6] H. Shirakawa, E.J. Louis, A.G. MacDiarmid, C.K. Chiang, and A.J. Heeger, JCS Chem. Commun. **16**, 578 (1977).
[7] F. Garnier, R. Hajlaoui, A. Yassar, and P. Srivastava, Science **265**, 1684 (1994).
[8] R.H. Friend, R.W. Gymer, A.B. Holmes, J.H. Burroughes, R.N. Marks, C. Tailiani, D.D.C. Bradley, D.A. Dos Santos, J.L. Brédas, M. Lögdlund, and W.R. Salaneck, Nature (London) **397**, 121 (1999).
[9] P.-M. Allemand, K.C. Khemani, A. Koch, F. Wudl, K. Holczer, S. Donovan, G. Gruner, and J.D. Thompson, Science **253**, 301 (1991).
[10] A. Rajca, J. Wongsriratanakul, and S. Rajca, Science **294**, 1503 (2001).
[11] A. Mielke and H. Tasaki, Commun. Math. Phys. **158**, 341 (1993).
[12] H. Tasaki, Prog. Theor. Phys. **99**, 489 (1998).
[13] E.H. Lieb, Phys. Rev. Lett. **62**, 1201 (1989).
[14] Mataga has studied a model for ferromagnetic polymer, see, e. g., N. Mataga, Theor. Chim. Acta **10**, 372 (1968).
[15] N. Shima and H. Aoki, Phys. Rev. Lett. **71**, 4389 (1993).
[16] A. Mielke, J. Phys. A **24**, 3311 (1991).
[17] A. Mielke, J. Phys. A **25**, 4335 (1992).
[18] A. Mielke, Phys. Lett. A **174**, 443 (1993).
[19] H. Tasaki, Phys. Rev. Lett. **69**, 1608 (1992).
[20] H. Tasaki, J. Stat. Phys. **84**, 535 (1996).
[21] H. Sakamoto and K. Kubo, J. Phys. Soc. Jpn. **65**, 3732 (1996).
[22] R. Arita, K. Kuroki, H. Aoki, A. Yajima, M. Tsukada, S. Watanabe, M. Ichimura, T. Onogi, and T. Hashizume, Phys. Rev. B **57**, R6854 (1998).
[23] R. Arita and H. Aoki, Phys. Rev. B **61**, 12 261 (2000).
[24] K. Penc, H. Shiba, F. Mila, and T. Tsukagoshi, Phys. Rev. B **54**, 4056 (1996).
[25] J.P. Perdew, K. Burke, and Y. Wang, Phys. Rev. B **54**, 16 533 (1996).
[26] D. Vanderbilt, Phys. Rev. B **41**, 7892 (1990).

[27] K. Laasonen, A. Pasquarello, R. Car, C. Lee, and D. Vanderbilt, Phys. Rev. B **47**, 10 142 (1993).
[28] R. Arita, Y. Suwa, K. Kuroki, and H. Aoki, Phys. Rev. Lett. **88**, 127202 (2002).
[29] J.-O. Lee, G. Lientschnig, F. Wiertz, M. Struijk, R.A.J. Janssen, R. Egberink, D.N. Reinhoudt, P. Hadley, and C. Dekker, Nano-Lett. **3**, 113 (2003).
[30] Y. Muraoka and Z. Hiroi, J. Phys. Soc. Jpn. **72**, 781 (2003).
[31] R. Arita, Y. Suwa, K. Kuroki, and H. Aoki, Phys. Rev. B **68**, 140403(R) (2003).